Outphasing Class-E/F_2 Power Amplifier using a Quadrature Hybrid as Non-Isolating Combiner

Ana Cordero, M. Nieves Ruiz, David Vegas, José A. García
Department of Communications Engineering, University of Cantabria, 39005 Santander, Spain

***Abstract*— This paper presents a GaN HEMT outphasing power amplifier (PA), based on a class-E/F_2 topology with reduced sensitivity to variable resistive load operation, designed to provide output power control over an extended range with high efficiency. A 90-degree hybrid coupler is used as non-isolating combiner, incorporating an appropriate reactive termination on its fourth port. Besides its many intrinsic advantages, the mutual load modulation trajectories may be rotated by simply adjusting a capacitor value or alternatively the length of an open-circuited transmission line. Once implemented at UHF band, the outphasing PA provides a drain efficiency higher than 70% up to an output power 10 dB below its peak value (42.2 dBm).**

Keywords*— *class-E, Chireix, load modulation, load-pull, outphasing, power amplifier, power efficiency.

I. Introduction

As modern wireless systems advance in the use of complex modulation schemes to accommodate high-data rates within restricted frequency bands, the design of power efficient transmitter architectures is more challenging than ever so as to handle such spectrally efficient signals with unprecedented peak-to-average power ratio (PAPR) values. Forcing the power consumption to follow the envelope of the signal, thanks to dynamic load modulation and/or dynamic biasing techniques [1], good average efficiency figures may be possible while also satisfying stringent linearity requirements.

Outphasing is one of the techniques that have been receiving increased attention, particularly since the introduction of highly efficient class-E PAs [2]. Exploiting the potential of its continuous modes [3], the power range to be covered with low losses may be extended beyond the 8-9 dB output power back-off (OPBO) limit typical of single load modulating techniques. In [4], the authors combined these concepts in a lumped element class-E/F_2 topology for the UHF band. Integrating two of those PAs with a series combiner and an impedance transformer, a 12.2 dB PAPR 10 MHz LTE signal was reproduced with an average efficiency above 45%. Due to the narrowband nature of the Chireix architecture, attention is being paid to multi-band or reconfigurable topologies [5]. Interest has also appeared on its combination with the Doherty technique [6] in order to achieve very high efficiency over a much larger OPBO range.

In a Doherty amplifier, an impedance inverter based on a quadrature hybrid coupler (QHC) [7] may provide operational advantages and may be simpler to implement than the classical solution with quarter-wavelength lines. Surface-mounted commercially available parts, fabricated with higher dielectric constant materials, can be physically smaller. A quadrature coupler may not only lead to a wider bandwidth response but it may also allow the extension of the topology to low frequency bands in which transmission lines use to be prohibitive. Although these couplers are often found as isolating combiners in balanced PAs or LINC transmitters [8], an outphasing alternative with improved linearity but extremely poor efficiency when handling high PAPR signals, their use as non-isolating combiners is not that common.

In this paper, two GaN HEMT class-E/F_2 PAs are integrated with a reactively terminated 90-degree hybrid coupler in an outphasing scheme for UHF band operation. Besides providing a competitive efficiency versus output power profile, the reactive termination allows rotating the mutual load modulation trajectories for a simple readjustment with potential for frequency reconfiguration.

II. Load-Independent Class-E/F_2 PA

A. Device Characterization and Load-pull Contours

A packaged GaN HEMT device from WolfSpeed, CGH35030F, was selected for the design. A very good estimate for the equivalent device output capacitance, C_{out} = 3.21 pF at 700 MHz, may be extracted from the value of the S_{22} parameter (included in Fig. 1) with the device biased at the selected point. The drain DC voltage, V_{DS} = 16 V, avoids the peak in the drain-to-source voltage waveform to reach the breakdown voltage in the worst operating condition, while the gate DC voltage, V_{GS} = -3.4 V, was adjusted just below the value for which some increase in the output conductance could be appreciated. A marker in Fig. 1 provides the S_{22} value at the frequency of the second harmonic, 1.4 GHz.

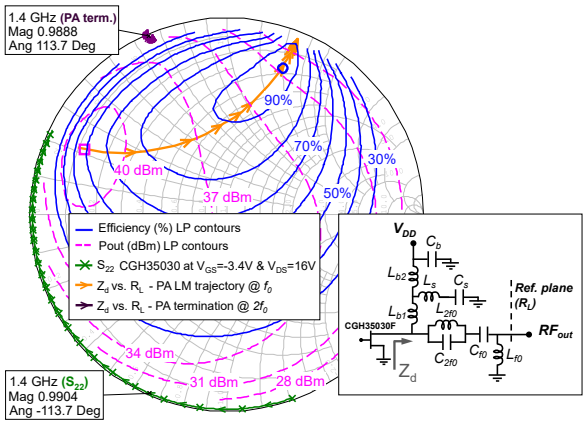

Fig. 1. Simulated load-pull (LP) contours with the sinthesized LM trayectory at 700 MHz and the 1.4 GHz termination. The S_{22} parameter of the CGH35030F GaN HEMT has been also added. The inset shows the schematic of the selected output network for the class-E/F_2 UHF PA.

After adjusting the CW input power level to approximate a switch-mode of operation, load-pull simulations at the fundamental, f_0, were completed (see Fig. 1) for a nearly infinite choke, a 1∠113.7º reflective termination at the second harmonic and open circuit conditions at the higher order ones, corresponding to those for a class-E/F$_2$ amplifier [3]. An optimum load modulating (LM) trajectory exists [4], including the impedance points providing maximum efficiency for each output power level. Under theoretical assumptions, a 100% efficiency vs. output power profile would result from zero but variable slope voltage switching operation.

B. *Drain Terminating Network*

The selected class-E/F$_2$ topology [4] is shown in Fig. 1 inset. With the $L_{2f0}C_{2f0}$ and L_sC_s circuits tuned at 1.4 GHz, L_{b1} is responsible for providing the 1∠113.7º termination required for resonating C_{out} at $2{\cdot}f_0$. L_{b2} was adjusted in order to force the drain biasing network to act as a RF choke at 700 MHz. C_{f0} and L_{f0} allow synthesizing the desired LM trajectory at the fundamental. This trajectory and the $2{\cdot}f_0$ termination were added to Fig. 1.

III. 90° Hybrid Coupler as Chireix Combiner

A QHC may be employed as a Chireix combiner if reactively terminating the port isolated from the output, which is usually loaded with the nominal impedance Z_0, as depicted in Fig. 2a. Using a $-j{\cdot}X_{term}$ = -j·50 Ω capacitive termination, the impedance values at the input ports, RFin$_1$ and RFin$_2$, describe horizontally oriented trajectories centered along the resistive axis over the Smith Chart (see Fig. 2b), when varying the outphasing angle, $\Delta\theta$, between the applied CW voltage waveforms, $v_{RFin1}(t)$ and $v_{RFin2}(t)$, in eqs. (1a) and (1b). V_{RF} denotes the amplitude and ω_0 the design angular frequency.

$$v_{RFin_1}(t) = V_{RF} \cdot cos\left[\omega_0 \cdot t + \frac{\Delta\theta}{2} + 90^\circ\right] \quad (1a)$$

$$v_{RFin_2}(t) = V_{RF} \cdot cos\left[\omega_0 \cdot t - \frac{\Delta\theta}{2}\right] \quad (1b)$$

The compensating reactances, $-j{\cdot}X_{comp}$ and $j{\cdot}X_{comp}$, play their typical role in a Chireix combiner, adjusting the imaginary component of the input impedance and the $\Delta\theta$ values for which a pure resistance may be synthesized. If terminated with an open-circuited transmission line (OCTL), as in Fig. 2c, the electrical length value, EL, should be adjusted to 45º attending to eq. (2a). Similar trajectories are possible when inductively terminating the isolated port with $j{\cdot}X_{term}$ = j·50 Ω. The position of the compensating capacitor and inductor should be interchanged, while the sign of the $\Delta\theta/2$ terms in eqs. (1a) and (1b) should be switched. A short-circuited transmission line (SCTL) of similar electric length may be valid from eq. (2b) if interested in a distributed implementation of the inductive termination.

$$Z_{term} = -j \cdot Z_0 \cdot cot(\beta \cdot l) \quad (2a)$$

$$Z_{term} = j \cdot Z_0 \cdot \tan(\beta \cdot l) \quad (2b)$$

with $$\beta \cdot l = \frac{EL}{180} \cdot \pi \quad (2c)$$

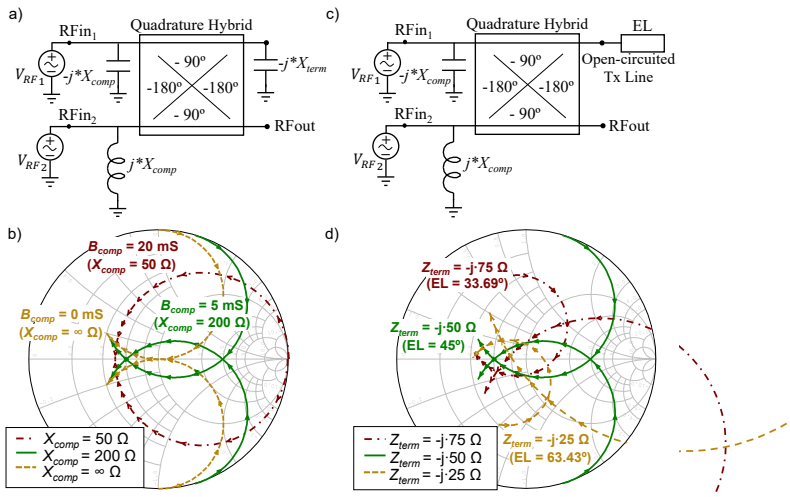

Fig. 2. QHC-based Chireix combiner with a) a capacitor and c) an OCTL reflective termination ($V_{RF1} = j{\cdot}V_{RF}{\cdot}e^{(j\cdot\Delta\theta/2)}$ and $V_{RF2} = V_{RF}{\cdot}e^{(-j\cdot\Delta\theta/2)}$). Input impedance evolution for a $\Delta\theta$ sweep from -90º to 90º as a function of b) X_{comp} for Z_{term} = -j·50 Ω, and as a function of d) Z_{term} for X_{comp} = 200 Ω.

Besides the intrinsic operational and implementation advantages offered by the use of a quadrature hybrid coupler in section I, the input impedance loci may be easily rotated if properly varying the value of the reactive termination, as represented in Fig. 2d. This simple tool would allow an accurate readjustment of the circuit after fabrication or could be exploited for frequency reconfiguration if wideband constituting PAs were employed instead.

IV. Class-E/F$_2$ Outphasing Amplifier

If integrating the multi-harmonic output network in Fig. 1 for each class-E/F$_2$ PA with the QHC-based combiner in Fig. 2a, the impedance loci at the combiner inputs are moved from the horizontal orientation in Fig. 2b to a position centered along the LM trajectory represented in Fig. 1 [2, 4]. In this way, the outphasing angle could offer control over the drain impedance at the fundamental in the desired region over the LP contours. As a consequence, a highly efficient operation along a large output power back-off range could be possible.

The 11304-3S surface mounted QHC from Anaren Inc., covering the 500-1000 MHz band, was selected for the design. Due to some amplitude and phase unbalance, the mutual LM trajectories as seen from the device drain terminals were slightly shifted apart from the desired position, as observed in Fig. 3. With a reduction of 0.2 pF in the value of the QHC terminating capacitor, the loci could be easily readjusted in simulation in order to guarantee the highest possible efficiency at the high impedance or deep OPBO side.

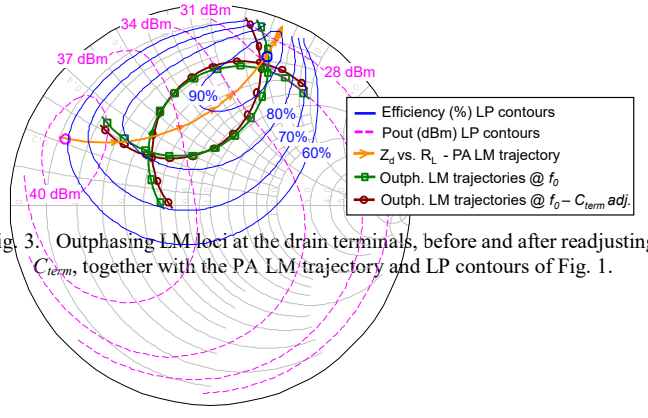

Fig. 3. Outphasing LM loci at the drain terminals, before and after readjusting C_{term}, together with the PA LM trajectory and LP contours of Fig. 1.

A. Implementation

The final schematic and a photograph of the implemented outphasing architecture are shown in Fig. 4. Notice that the Chireix compensating susceptances have been incorporated into the output networks of the class-E/F_2 PAs. The series capacitor and the parallel LC circuit to ground contributed to synthesizing the desired drain impedance at the fundamental in both PA networks despite some differences imposed by the PCB. The required pads for soldering the QHC determined the need for using a much smaller terminating capacitor than the one predicted by simulation. High-Q air-core coils and multilayer ceramic capacitors, from Coilcraft and ATC respectively, were employed. The bank of high-valued capacitors in each biasing path was not included in the schematic for simplicity. The connector in the isolated port was added to allow adjusting and testing an alternative open-circuited microstrip termination.

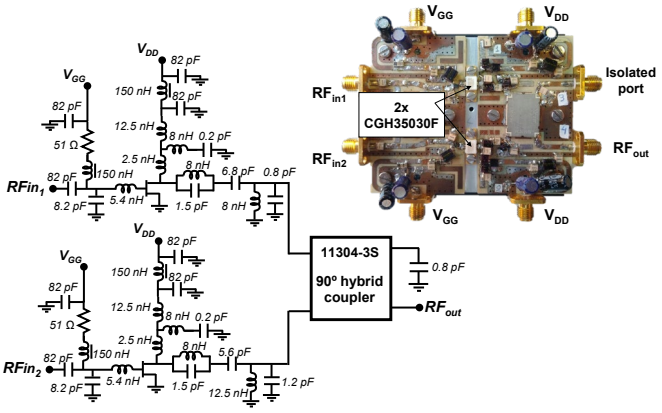

Fig. 4. Implemented outphasing topology: schematic and photograph.

B. Measured Results

The class-E/F_2 Chireix amplifier was finally characterized as a function of the outphasing angle between the CW driving signals. The measured efficiency versus output power profiles at different frequencies are included in Fig. 5a. A peak efficiency value higher than 75% was measured at the central frequency, f_0, for 8.5 dB of output power back-off. The drain efficiency stays above 70% and 50% at 10 dB and 11.8 dB of output power back-off, respectively. Although the resulting f_0 was slightly shifted (2.7%) below the design central frequency, mainly due to the difference between the device and the model equivalent C_{out}, the performance is as expected.

Fig. 5b shows the measured efficiency and peak output power versus frequency at different power back-off levels. As it may be appreciated, the efficiency remains higher than 50% at 10 dB OPBO in a bandwidth around 18 MHz while it is above 63.5% at 8 dB OPBO in the whole range. The peak output power changes less than 0.5 dB in the measured frequency range, with a maximum of 42.4 dBm at the low frequency edge.

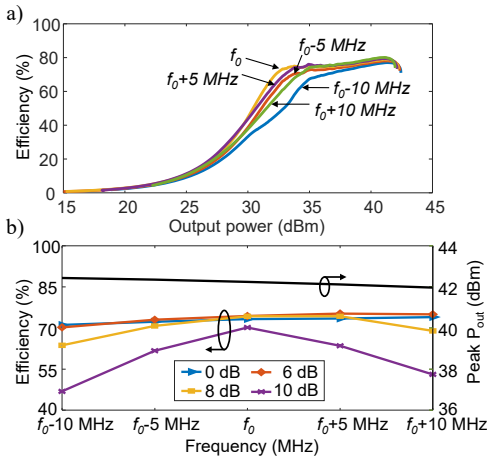

Fig. 5. a) Measured drain efficiency versus output power profiles at different frequencies. b) Measured peak output power and efficiency values at different OPBO levels (0–10 dB) as a function of frequency.

V. Conclusion

A GaN HEMT outphasing amplifier, based on a load-insensitive class-E/F_2 topology and a non-isolating combiner designed over a quadrature hybrid coupler, has been presented. Besides its intrinsic advantages, the employed combiner allows rotating the mutual load modulation trajectories by simply adjusting a capacitor value or alternatively the length of an open-circuited transmission line. Once implemented at the 700 MHz LTE band, the outphasing PA provides an efficiency higher than 70% up to an output power 10 dB below its peak. Compared to some state-of-the-art outphasing PAs in table I, the proposed solution offers a competitive performance with small footprint.

TABLE I
Comparison With GaN State-of-the Art Outphasing PAs

Ref.	f_0 *(GHz)*	η_{peak}*(%)*	$\eta_{/0}$ @ 6dB/10 dB/13 dB (%)	P_{out_max} (W)	*Architecture*
[6]	0.58	77.7	68 / 74 / 66	132	Doherty-Outphasing
[4]	0.7	70	66.4 / 66.7 / 64	47.75	Outphasing
This work	**0.7**	**75.1**	**74.4 / 70 / 35.4**	**17.4**	Outphasing
[9]	0.9	≈82	≈80 / ≈70 / ≈37	24	Outphasing
[10]	1.95	77	70 / 65 / ≈40	19	Outphasing
[11]	2.14	66	58 / 56 / 43	112	Doherty-Outphasing

Acknowledgment

This work was supported by the Spanish Ministry of Science, Innovation and Universities through TEC2017-83343-C4-1-R project, co-funded with FEDER. D. Vegas also thanks for the BES-2015-072203 grant.

References

[1] F. H. Raab *et al.*, "Power amplifiers and transmitters for RF and microwave," *IEEE Trans. Microwave Theory Tech.*, vol. 50, no. 3, pp. 814-826, Mar 2002.

[2] R. Beltran, F. H. Raab and A. Velazquez, "HF outphasing transmitter using class-E power amplifiers," *IEEE MTT-S Int. Microw. Symp. Dig.*, Boston, MA, USA, June 2009, pp. 757-760.

[3] S. D. Kee *et al.*, "The class-E/F family of ZVS switching amplifiers," *IEEE Trans. Microwave Theory Tech.*, vol. 51, no. 6, pp. 1677-1690, June 2003.

[4] D. Vegas, J. Perez-Cisneros, M. N. Ruiz and J. A. García, "UHF class E/F_2 outphasing transmitter for 12 dB PAPR signals," *IEEE MTT-S Int. Microw. Symp. (IMS)*, Boston, MA, USA, June 2019.

[5] D. N. Martin *et al*., "An 18-38-GHz K-/Ka-band reconfigurable Chireix outphasing GaAs MMIC power amplifier," *IEEE Trans. Microwave Theory Tech.*, vol. 68, no. 7, pp. 3028-3038, July 2020.

[6] A. Yamaoka, T. M. Hone and K. Yamaguchi, "70% efficient dual-input Doherty-outphasing power amplifier for large PAPR signals," *IEEE MTT-S Int. Microw. Symp. (IMS)*, Boston, MA, USA, June 2019.

[7] R. E. Mayer, K. W. Lho, L. F.Root, and E. W. Louis, "High efficiency amplifier," U.S. Patent 6.922.102 B2, Jul. 26, 2005.

[8] D. C. Cox, "Linear amplification with nonlinear components," *IEEE Trans. Comm.*, vol. COM-23, pp. 1942–1945, Dec. 1974.

[9] M. Özen, M. van der Heijden, M. Acar, R. Jos, and C. Fager, "A Generalized Combiner Synthesis Technique for Class-E Outphasing Transmitters," *IEEE Trans. Circuits Syst. I, Reg. Papers*, vol. 64, no. 5, pp. 1126–1139, May 2017.

[10] M. P. van der Heijden, M. Acar, J. S. Vromans and D. A. Calvillo-Cortes, "A 19W high-efficiency wide-band CMOS-GaN class-E Chireix RF outphasing power amplifier," *IEEE MTT-S Int. Microw. Symp.,* Baltimore, MD, 2011.

[11] A. R. Qureshi, M. Acar, J. Qureshi, R. Wesson and L. C. N. de Vreede, "A 112W GaN dual input Doherty-Outphasing Power Amplifier," *IEEE MTT-S Int. Microw. Symp. (IMS)*, San Francisco, CA, 2016.